

Criticality in the one-dimensional Kohonen neural map

István Csabai and Tamás Geszti

Department of Atomic Physics, Eötvös University, Puskin utca 5-7, H-1088 Budapest, Hungary

Gábor Vattay

Department of Solid State Physics, Eötvös University, Múzeum krt. 6-8, H-1088 Budapest, Hungary

(Received 3 May 1992)

In the marginally stable ordered state of Kohonen's feature-map neural-network model the distribution of fluctuating distances between neighboring cells is found to be a self-similar Weierstrass-Mandelbrot-type function with a nontrivial scaling exponent. The relationship among the quantities describing the distribution is discussed in terms of a balance between a deterministic multiplicative and a stochastic additive process, described by a Perron-Frobenius operator. Two regions of the Kohonen learning parameter α , separated by $\alpha_c \approx 0.63$, differ in the character of both fluctuation and ordering, the latter being fastest close to α_c .

PACS number(s): 87.10.+e, 05.40.+j, 05.45.+b, 05.70.Jk

Kohonen's feature map [1] is an adaptable quasineural mapping of a continuous vectorial input \mathbf{x} onto a discrete output \mathbf{i}^* , interpreted as the index vector of one (the "winner") of a set of neurons, labeled by index i . Each neuron carries a continuous vectorial "weight" \mathbf{w}_i , and the winner is selected by having its weight closest (e.g., in Euclidean distance) to the input. The mapping can be adapted to a particular task by changing the weights. Biological motivation for discretizing through winner selection comes from the existence of layers of neurons doing parallel feed-forward processing and competing by mutual lateral inhibition, present in various parts of the brain processing sensory information, e.g., in the visual cortex. In what follows we restrict ourselves to the one-dimensional model.

The particular task posed for Kohonen's feature map—motivated by the way an infant learns to see—is to make the mapping topologically correct, i.e., to assign neighboring outputs to nearby inputs. This global aim is achieved by a self-organizing process that consists in iterating the following steps of adaptation [1]:

(i) Generate a random input x out of a given distribution [in our case: uniform on interval $(0, 1)$] and select the corresponding winner i^* , as stated above, by

$$|x - w_{i^*}| = \min_i |x - w_i|. \quad (1)$$

(ii) Modify the weights of the winner and its index neighbors through

$$w_i(t+1) = w_i(t) + \alpha(i - i^*)[x - w_i(t)]. \quad (2)$$

The function $\alpha(d)$ is the amplitude of the adaptation. It is usually a bell-shaped function of the distance $|i - i^*|$. In practical applications its range and amplitude decrease with the discrete time t , for reasons analogous to simulated annealing [2]. In the present work we restrict ourselves to nearest-neighbor interaction [$\alpha(d) = 0$ for $|d| > 1$], constant in time.

It is easy to see that the above learning rule orders the weights into one of two spontaneously symmetry-breaking states: either monotonously increasing,

$$w_1 \leq w_2 \leq \dots \leq w_N, \quad (3)$$

or monotonously decreasing,

$$w_1 \geq w_2 \geq \dots \geq w_N. \quad (4)$$

The ordered states are stable after the system reached one of them [3], under the condition [4] that $\alpha(d)$ should decrease monotonously with the distance $|d|$. In this sense $\alpha(0) = \alpha(\pm 1) = \alpha$ is a one-parameter boundary of stability, along which one expects critical fluctuations. That motivated the present study, directed at that critical line.

After the ordering process is completed, the distances $|w_{i+1} - w_i|$ between the weights still fluctuate due to the local dynamics. In the following we focus our attention on this stationary behavior.

The fluctuations can be characterized by the distribution $\varrho(s_i)$ of the rescaled distances

$$s_i = N |w_{i+1} - w_i|, \quad (5)$$

which is independent of N . Disregarding boundary effects, this density function is the same for all i 's. Our simulations show that it is not a simple bell-shape function around the mean distance $\bar{s} = 1$ [Figs. 1(a) and 1(b)]. For large distances, the distribution decays exponentially, due to the 'thermal' fluctuations of a quantity obeying a local conservation law (distance is exchanged between neighbors).

For small s the distribution shows scaling behavior. Its envelope is a power function $s^{D(\alpha)}$ with its exponent depending on the amplitude of adaptation α . For $\alpha < \alpha_c \approx 0.63$ the exponent $D(\alpha)$ is positive [Fig. 1(a)], describing two neighboring weights that repel each other, while for $\alpha > \alpha_c$ it is negative [Figs. 1(b) and 2], corresponding to an effective attraction between neighboring

weights. In the second case the distribution $\rho(s)$ has an inherent Weierstrass-Mandelbrot-type structure [5, 6] consisting of a self-similar sequence of Poissonian-shaped peaks $\rho_0(s)$ embedded in the power singularity:

$$\rho(s) \approx \sum_{l=0}^{\infty} c_2^l \rho_0(c_1^l s), \quad (6)$$

where c_1 and c_2 are stretching factors.

The emergence of the self-similar distribution can be traced back to the random alteration of multiplicative shrinking by a fixed ratio, and additive stretching by a stochastic increment. Indeed, the distance between

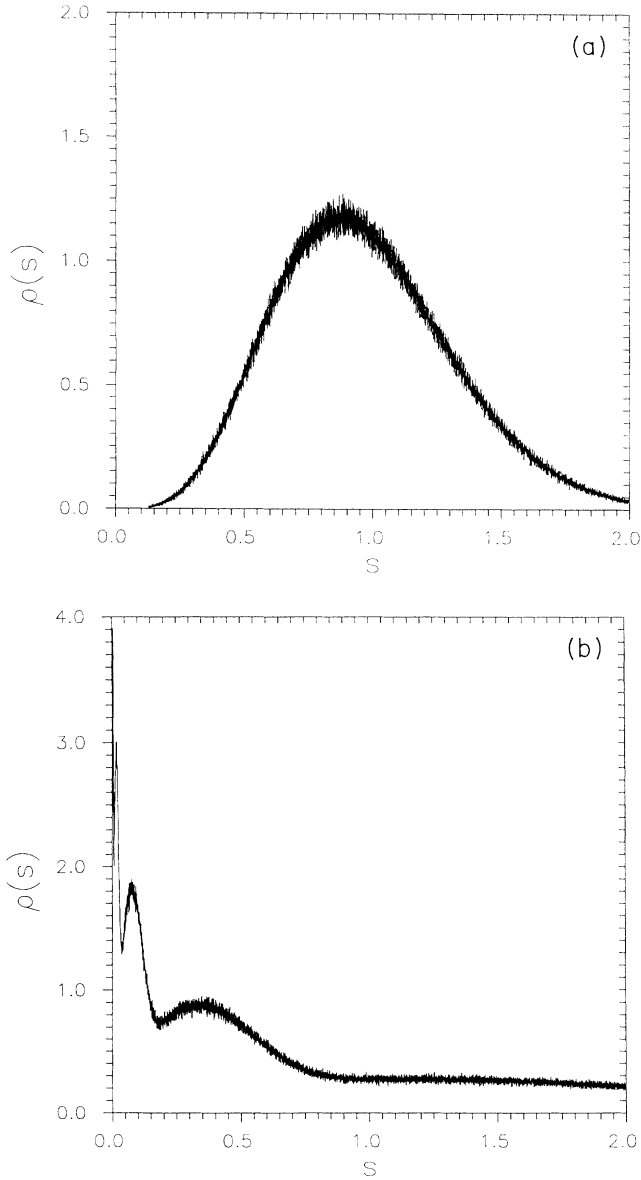


FIG. 1. The distribution of the distance between the weights of two neighboring neurons. The number of iteration steps was 2×10^7 , starting from an initially ordered state of $N = 20$ cells. The amplitude of adaptation was (a) $\alpha = 0.2$ and (b) $\alpha = 0.8$. The small- s behavior is highly different below (a) and above (b) the critical value $\alpha_c \approx 0.63$.

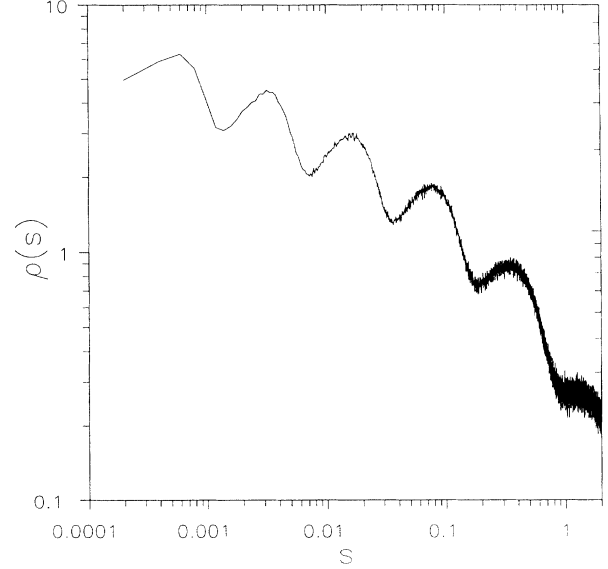


FIG. 2. The same as Fig. 1(b) on log-log scale. The repetition of peaks on smaller and smaller scales shows the Weierstrass-Mandelbrot structure of the distribution.

two given weights w_i and w_{i-1} can change according to Eq. (2) in two different cases: if one of them is the winner, or one of their neighbors w_{i+1} and w_{i-2} is. From Eq. (2) one can derive the respective changes of the distances and we get in the first case

$$s(t+1) = (1 - \alpha)s(t), \quad (7)$$

whereas in the second case we obtain

$$s(t+1) = s(t) + \alpha\xi, \quad (8)$$

where ξ is the distance between the stochastic input and the winner. Its distribution $P(\xi)$ is also “Poissonian-like” since it is generated by a process similar to the dynamics of the spacings. The presence of a deterministic component (7) and a stochastic one (8) in the Kohonen map can be demonstrated directly by plotting $s(t+1)$ against $s(t)$ when a distance is updated (Fig. 3).

The relative probabilities of the two kinds of events (7) and (8) depend slightly on the distance s and are denoted by $p(s)$ and $1 - p(s)$, respectively. In the small- s limit the value of $p(s)$ is near to $1/3$ since the ratio of the intervals where w_i or w_{i-1} and w_{i+1} or w_{i-2} is the winner is approximately 1:2.

The approximation $p(s) \approx p = 1/3$, valid for $s \rightarrow 0$, decouples the dynamics of the first-neighbor distance from the rest of the system. The distribution generated by iterating Eqs. (7) and (8) taken in random alteration with the respective probabilities $1/3$ and $2/3$ is an efficient mean-field-like model reflecting the main properties of the original system: the shape of the distribution, and the exponential decay of the large- s tail.

In what follows we consider that simplified model, open to analytical description by means of a self-consistent Perron-Frobenius (PF) equation that already proved useful for spatially extended models decoupled in an analo-

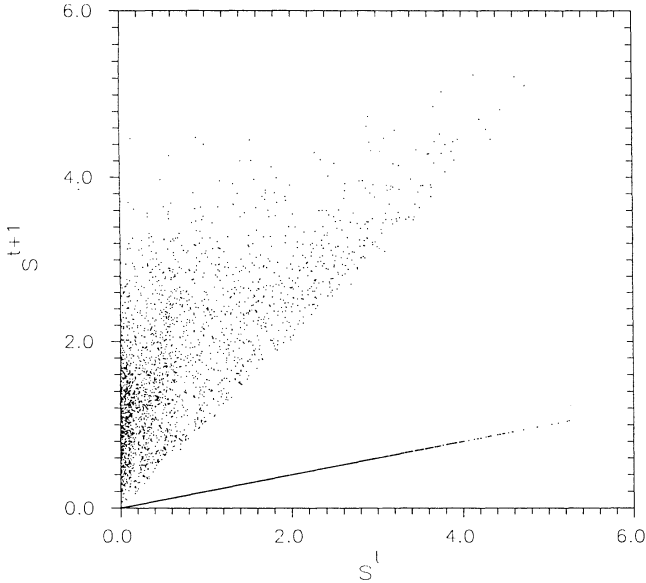


FIG. 3. $s(t+1)$ vs $s(t)$ for one pair of neighboring cells in the full Kohonen model at $\alpha = 0.8$ after 5000 iteration steps. The coexistence of a pure deterministic and a stochastic component of the dynamics is apparent.

gous way [7]. The PF equation for the one-body distribution reads

$$\varrho(s) = \frac{p}{1-\alpha} \varrho(s/(1-\alpha)) + (1-p) \int \varrho(s-\alpha\xi) P(\xi) d\xi. \quad (9)$$

That allows us to extract the power singularity of the distribution in $s = 0$. Indeed, in that limit we can neglect the second term on the right-hand side; then we get

$$\varrho(s) = \frac{p}{1-\alpha} \varrho(s/(1-\alpha)). \quad (10)$$

This equation is apparently solved by a self-similar function of the form of Eq. (6) (apart from the $l = 0$ term), with $c_1 = 1/(1-\alpha)$ and $c_2 = p/(1-\alpha)$. An independent solution is the envelope $\varrho(s) = s^{D(\alpha)}$, where the exponent $D(\alpha)$ is fixed by Eq. (10) through

$$D(\alpha) = \frac{\ln p}{\ln(1-\alpha)} - 1. \quad (11)$$

Equation (11) is our main result obtained from the effective dynamics of the decoupled model. Now we compare it with the original Kohonen map. In Fig. 4 we plotted $D(\alpha)$ versus $1/\ln(1-\alpha)$, measured in the Kohonen model. We find excellent agreement with formula (11) if we set $p = 0.37 \pm 0.01$, which is not far from our rough estimate $1/3$. Equation (11) also tells us the critical value of α_c where the first-neighbor repulsion-attraction transition occurs. The equation

$$D(\alpha_c) = 0 \quad (12)$$

yields $\alpha_c = 1 - p \simeq 0.63 \pm 0.01$ in accordance with the simulations (see above).

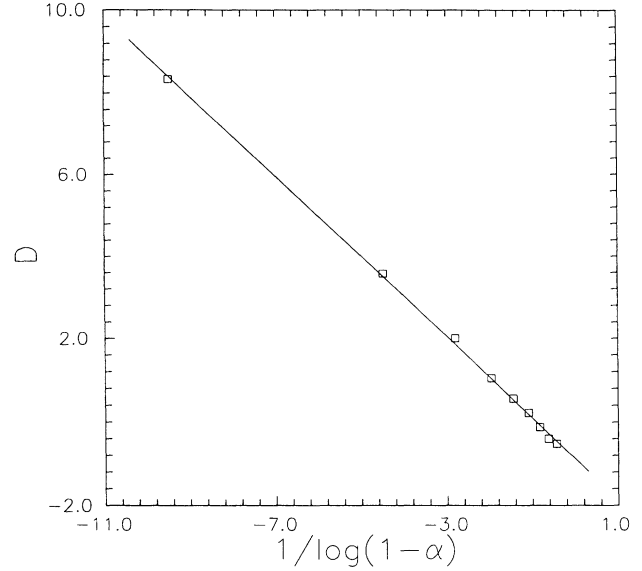


FIG. 4. The measured exponent (squares) D as the function of $1/\ln(1-\alpha)$. The slope of the linear fit (solid line) gives $\ln(p) = -0.98$.

So far we have concentrated on critical fluctuations in the marginally stable topologically ordered state. A clarification of the ordering process itself can be of use for practical applications of the Kohonen map. Along the stability boundary of the one-dimensional, nearest-neighbor Kohonen map studied in the present paper, Fig. 5 shows the ordering time T_{ord} (number of steps needed to reach an ordered state from a random one) as a function of α . The fastest ordering is observed close to α_c , which seems to separate two regions of different mechanisms of ordering. For $\alpha < \alpha_c$ we observe $T_{\text{ord}} \propto \alpha^{-1}$, which is

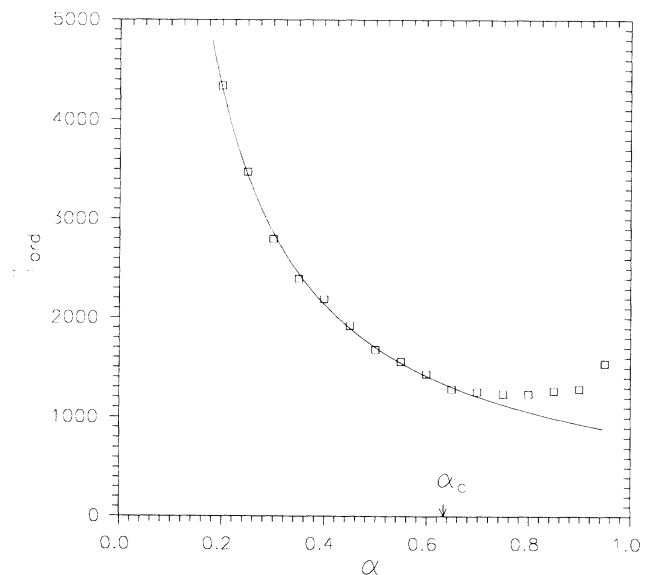


FIG. 5. The time needed for ordering from a random initial condition (average over 1000 runs). A const/α line fits well for $\alpha < \alpha_c$. The minimum of T_{ord} is close to α_c .

the “normal” behavior expected for a systematic, nondiffusive drift of topological defects towards the boundary of the sample [4]. On the other hand, for $\alpha > \alpha_c$ a localizationlike behavior seems to set in and T_{ord} increases as $\alpha \rightarrow 1$. Let us mention that the corresponding clustering of neurons may give rise to a hierarchical classification of data sets not having that structure.

The practical implications, perhaps relevant to off-criticality, for several dimensions too, may be the existence of optimal values of the Kohonen updating param-

eters to assure fastest topological ordering. In the final stage of a practical calculation the amplitude of adaptation is commonly reduced in time anyway, in order to reach a smooth final state.

We are indebted to I. Jánosi and F. Czakó for helpful cooperation on Fig. 3. This work was partly supported by the Hungarian Academy of Sciences (OTKA 2179 and OTKA 2090) and the New Wave Foundation.

[1] T. Kohonen, *Self-Organization and Associative Memory*, 2nd ed. (Springer-Verlag, Berlin, 1988).
 [2] S. Kirkpatrick, C. D. Gelatt, and M. P. Vecchi, *Science* **220**, 671 (1983).
 [3] M. Cottrell and J. C. Fort, *Ann. Inst. Henri Poincaré* **23**, 1 (1987).

[4] T. Geszti, *Physical Models of Neural Networks* (World Scientific, Singapore, 1990).
 [5] B. Mandelbrot, *The Fractal Geometry of Nature* (Freeman, San Francisco, 1982).
 [6] T. Tél, *Z. Naturforsch.* **43A**, 1154 (1988).
 [7] K. Kaneko, *Prog. Theor. Phys.* **99**, 263 (1989).

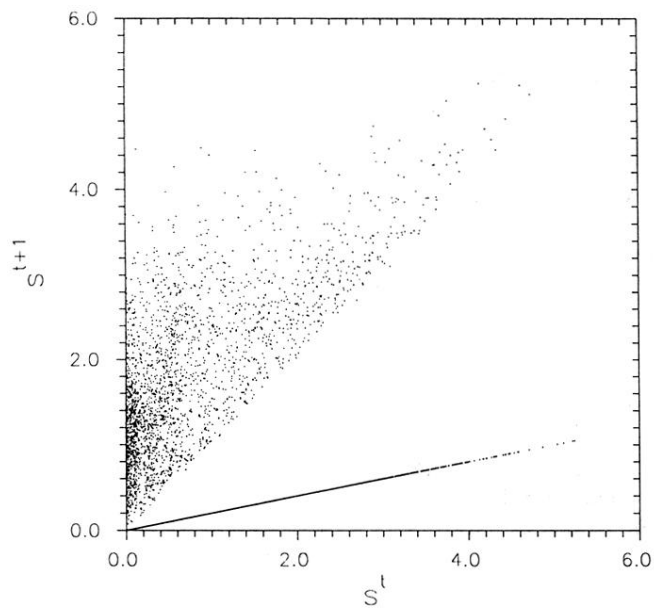


FIG. 3. $s(t+1)$ vs $s(t)$ for one pair of neighboring cells in the full Kohonen model at $\alpha = 0.8$ after 5000 iteration steps. The coexistence of a pure deterministic and a stochastic component of the dynamics is apparent.